Journal of the Korean Society
for Nondestructive Testing
Vol. 26, No. 3 (2006. 6)

Simulation and Analysis of ECT Signals Obtained at Tubesheet and Tube Expansion Area

Sung-Chul Song*, Yun-Tai Lee*, Hee-Sung Jung** and Young-Kil Shin**,†

Abstract Steam generator (SG) tubes are expanded inside tubesheet holes by using explosive or hydraulic methods to be fixed in a tubesheet. In the tube expansion process, it is important to minimize the crevice gap between expanded tube and tubesheet. In this paper, absolute and differential signals are computed by a numerical method for several different locations of tube expansion inside and outside a tubesheet and signal variations due to tubesheet, tube expansion and operating frequencies are observed. Results show that low frequency is good for detecting tubesheet location in both types of signals and high frequency is suitable for sizing of tube diameter as well as the detection of transition region. Also learned is that the absolute signal is good for measuring tube diameter, while the differential signal is good for locating the top of tubesheet and both ends of the transition region. In the case of mingled anomaly with tube expansion and tubesheet, low frequency inspection is found to be useful to analyze the mixed signal.

Keywords: Tubesheet, Tube Expansion, ECT, Absolute Signal, Differential Signal

1. Introduction

Steam generator tubes are expanded inside tubesheet holes. When a tube is expanded and fixed in a tubesheet hole, crevice gap may occur between the expanded tube and tubesheet. Crevice gap may be filled with by-products of corrosion, which eventually leads to denting and damages to tubes (Kong et al., 2004). Thus, it is important to minimize the crevice gap. The profilometry eddy current testing (ECT) signal has been used to examine the quality of tube expansion process. In this paper, absolute and differential signals are computed by the finite element method for several different locations of transition region inside and outside the tubesheet and signal variations due to tubesheet, tube expansion, and operating frequencies are observed.

Test conditions advantageous to find the top of tubesheet (TTS) and to recognize the transition region of tube diameter are investigated. In addition, several defect signals under the influence of tubesheet and tube expansion region are shown.

2. Finite Element Modeling

ECT is based on electromagnetic induction phenomena. If we assume sinusoidal steady state and perfect axisymmetry of tubes, tubesheet holes, and coils, the governing equation in cylindrical coordinate system can be written as follows:

$$\frac{1}{\mu}\left[\frac{\partial}{\partial\rho}\left\{\frac{1}{\rho}\frac{\partial}{\partial\rho}(\rho A)\right\}+\frac{\partial}{\partial z}\left\{\frac{1}{\rho}\frac{\partial}{\partial z}(\rho A)\right\}\right]-j\omega\sigma A+J_S=0 \qquad (1)$$

where μ, ω, σ, ρ, A, J_s are permeability, angular

Received: May 10, 2006, Accepted: May 29, 2006. * Sae-An Engineering Corp., Seoul 153-803, Korea, ** School of Electronic and Information Engineering, Kunsan National University, Kunsan, 573-701, † Corresponding author: ykshin@kunsan.ac.kr

frequency, conductivity, radial distance, magnetic vector potential, and source current density of coil, respectively. The term, $j\omega\sigma A$, is the eddy current density induced in a conducting material.

By applying the Galerkin's weighted residual method to the above equation and by using isoparametric quadrilateral elements, the following elemental matrix equations are obtained (Burnett, 1988).

$$([S]+j[C])\{A\}=\{Q\} \tag{2}$$

where elements of each matrix can be expressed as

$$S_{ij}=\int_{\Omega^e}\frac{1}{\mu}\left\{\left(\frac{N_i}{\rho}+\frac{\partial N_i}{\partial\rho}\right)\left(\frac{N_j}{\rho}+\frac{\partial N_j}{\partial\rho}\right)+\frac{\partial N_i}{\partial z}\frac{\partial N_j}{\partial z}\right\}2\pi\rho d\rho dz \tag{3}$$

$$C_{ij}=\int_{\Omega^e}\omega\sigma N_i N_j 2\pi\rho d\rho dz \tag{4}$$

$$Q_i=\int_{\Omega^e}J_s N_i 2\pi\rho d\rho dz \tag{5}$$

Here, N_i and N_j are shape functions at each node point in an element. These elemental matrix equations are summed up to form a global matrix equation and solved for the magnetic vector potential at every node point. The coil impedance can then be calculated by using the Faraday's law and Stoke's theorem. The resulting expression for the coil impedance is as follows:

$$Z=\frac{-j\omega\oint Adl}{\int_s J_s ds} \tag{6}$$

Since the impedance is a complex number, its horizontal and vertical components can be calculated. The subject of modeling is the Korean standard of nuclear power plant and the dimensions used are summarized in Table 1.

3. Display Methods and Prediction of Tube Expansion Signal

When tube diameter changes due to expansion, high operating frequency will give bigger signal. In this paper, such signals from high frequency are displayed following the calibration procedure of ASME code (ASME, 1986). However, tube expansion is made inside the tubesheet hole so that low frequency inspection is also necessary considering that the tubesheet is ferromagnetic. In this paper, 20 kHz signals are rotated so that the tubesheet signal is displayed vertically, which is the way of displaying a profilometry signal.

Fig. 1 shows horizontal and vertical components of absolute and differential signals when each probe passes the transition region. Horizontal axis in these figures indicates the sequence of moving probe position and the section between the 110th and the 200th positions corresponds to the transition region.

The two components of absolute signal change continuously in the transition region. The differential signal changes abruptly at both ends of transition region, but does not change much in the transition region. Differential signals do not return to zero value until the trailing coil completely gets out of the transition region. For these two types of signals, both horizontal and vertical components show bigger changes in the transition region as the frequency is increased. Signals displayed on the impedance plane do not rotate much and their amplitudes get bigger as the frequency increases.

Table 1 Dimensions used in the finite element modeling

	Before tube expansion	After tube expansion
Diameter of tubesheet hole	19.25 [mm]	19.25 [mm]
Thickness of SG tube	1.07 [mm]	1.069 [mm]
Tube outer diameter (OD)	19.05 [mm]	19.24 [mm]
Axial length of transition region	19.26 [mm]	

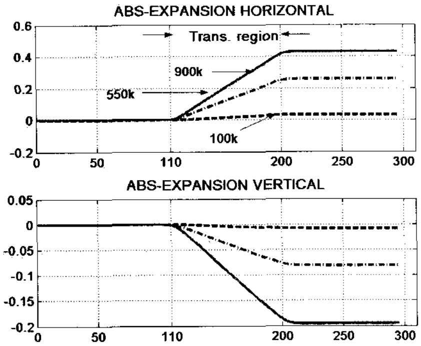

(a) Abs. signal

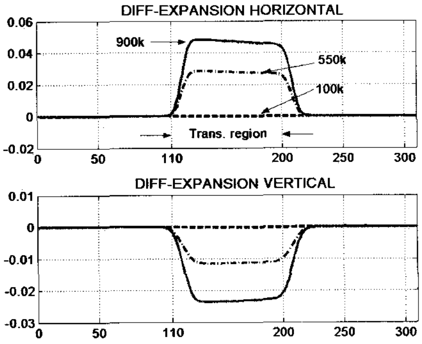

(b) Diff. signal

Fig. 1 Horizontal and vertical components of Abs. and Diff. signals

4. Signal Prediction at Tubesheet and Transition Region of Tube Diameter

After the tube expansion, it is necessary to inspect the relative position of transition region from the top of tubesheet (TTS). In this work, signals are predicted at 5 different tubesheet locations as shown in Fig. 2. Operating frequencies of 20, 100, 550, and 900 kHz are tested to find the advantageous test conditions to recognize TTS location and the transition region easily.

Identification of TTS.

Since the tubesheet is ferromagnetic and located outside the tube, low frequency inspection is necessary considering the skin effect phenomena. Fig. 3 compares magnetic flux contour plots of differential coil obtained by using 20 kHz and 900 kHz. Flux lines at low frequency reach TTS, but flux lines at high frequency do not reach TTS. Therefore, we can expect that low frequency is better for identifying TTS.

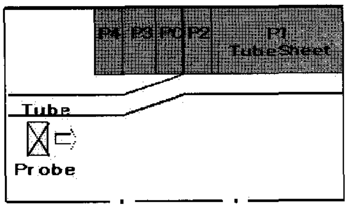

Fig. 2 Five different locations of TTS

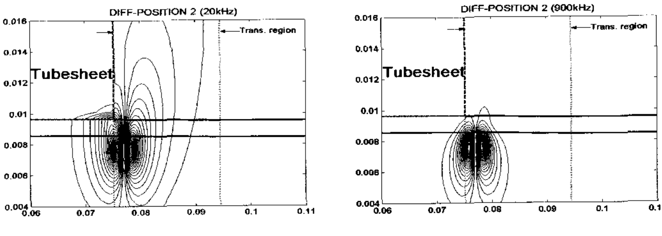

(a) 20 kHz (b) 900 kHz

Fig. 3 Contour plots of differential coil at 20 kHz and 900 kHz

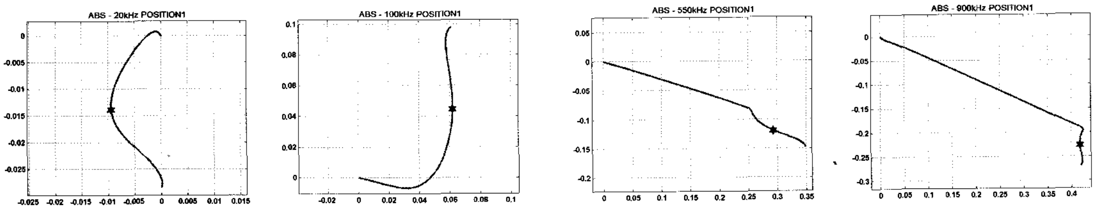

(a) 20kHz (b) 100kHz (c) 550kHz (d) 900kHz

Fig. 4 Absolute impedance plane signals when the tubesheet is at P1 position

Figs. 4 and 5 compare absolute impedance plane signals when the tubesheet is at P1 and P4 positions shown in Fig. 2. As the frequency increases, the signal part due to tubesheet rotates clockwise and becomes smaller, but the signal part due to transition region does not rotate and its size becomes increased. A star symbol (★) is marked in the signal as the probe passes TTS. If this symbol is located at the extreme right or left on the impedance plane signal, it would be possible to identify the TTS location from a horizontal component (profilometry) signal.

The horizontal and vertical components of absolute signal at 20 kHz are shown in Fig. 6(a). The horizontal component signals change suddenly at all points that the star symbol is marked. This means that the abrupt change in the horizontal component of absolute signal at 20 kHz indicates the exact location of TTS. Locating TTS is impossible if we use the vertical component signal or other frequencies. At 100 kHz as shown in Fig. 6(b), rough estimation of TTS location may be possible, but it will be very difficult since the peak point is not pronounced.

Fig. 7 shows differential impedance plane signals when the tubesheet is fixed at P4 position. The frequency dependent characteristics appeared in these signals are very similar to those in absolute signals. According to these figures, it may be possible to recognize TTS location at frequencies of 20, 100, and 900 kHz since the star symbol is located at the extreme right or left on the impedance plane signals. These observations are demonstrated in Fig. 8 where the horizontal and vertical components of Fig. 7 are shown. As a result, we learned that TTS identification is possible by noticing horizontal component of differential signals at 20, 100 and 900 kHz. At 900 kHz, the indication of TTS goes downward in the horizontal and vertical components of differential signal. This is because the signal part due to TTS appears vertically and in the downward direction in Fig. 7.

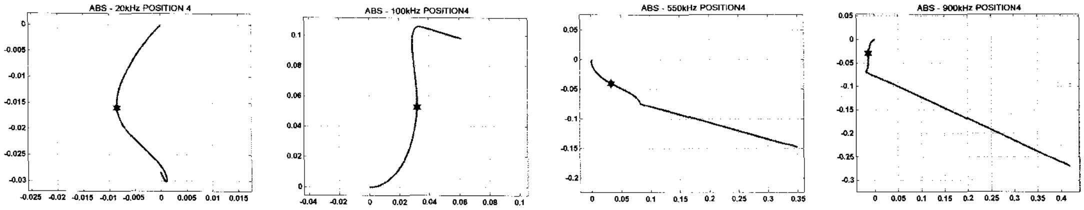

(a) 20kHz (b) 100kHz (c) 550kHz (d) 900kHz

Fig. 5 Absolute impedance plane signals when the tubesheet is at P4 position

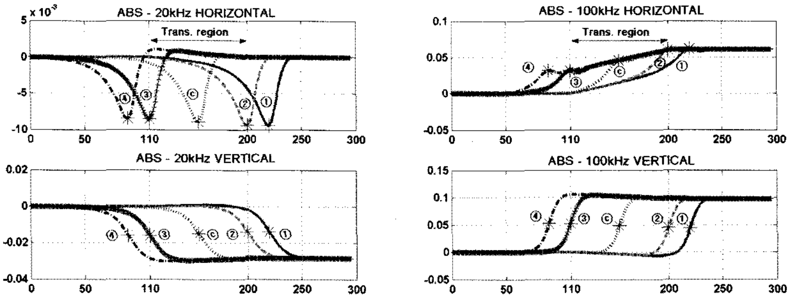

(a) Abs. 20kHz (b) Abs. 100kHz

Fig. 6 Horizontal and vertical components of absolute signals

Recognition of Transition Region of Tube Diameter

As the frequency increases, the effect of tube expansion on the absolute signal becomes bigger as shown in Fig. 9. At high frequencies, changes in horizontal component of absolute signal due to transition region are greater than those due to tubesheet. This will help us to recognize the transition region. The effect of tube expansion is smaller than those of tubesheet in the horizontal component of differential signal if 100 or 550 kHz is used. But, if 900 kHz is used, the effect of tubesheet is less than and opposite to those of transition region. Thus, the use of 900 kHz, differential signal would make it easier to recognize both the TTS location and the transition region.

Comparison of Absolute and Differential Signals

After the probe passes TTS or transition region, the value of absolute signal remains the same, but that of differential signal returns to zero. The signal variation due to tube expansion

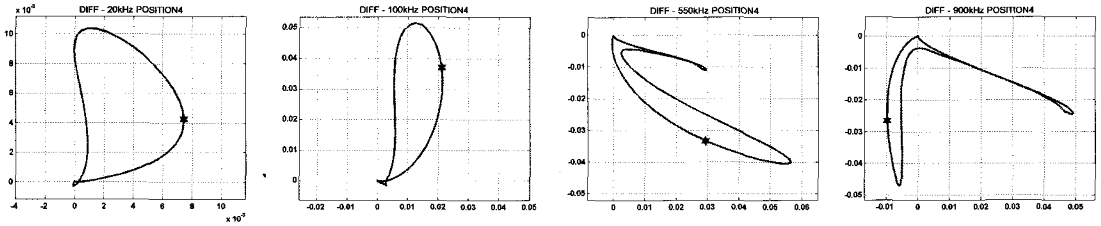

(a) 20kHz (b) 100kHz (c) 550kHz (d) 900kHz

Fig. 7 Differential impedance plane signals when the tubesheet is at P4 position

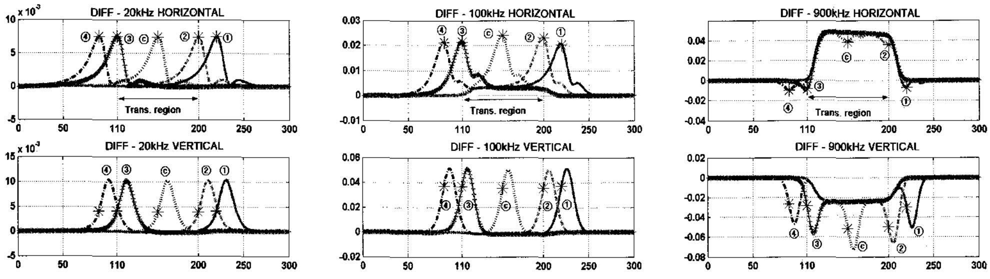

(a) 20kHz (b) 100kHz (c) 900kHz

Fig. 8 Horizontal and vertical components of differential impedance plane signals shown in Fig. 7

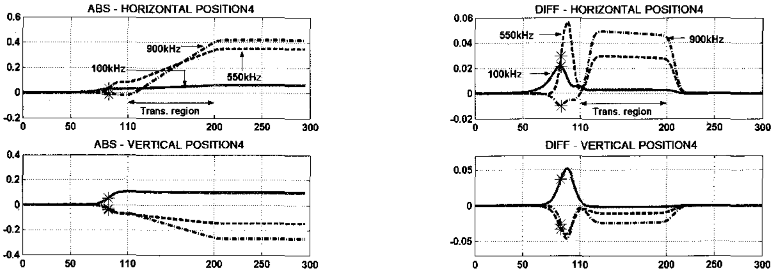

(a) Absolute signal (b) Differential signal

Fig. 9 Horizontal and vertical components of absolute and differential signals when the tubesheet is at P4 position is bigger and continuous in the absolute signal. This type of signal would be good for the measurement of expanded tube diameters. The differential signal changes suddenly when the probe sees abrupt changes in test environment. Thus, this type of signal would be good for locating TTS and both ends of the transition region of tube diameter.

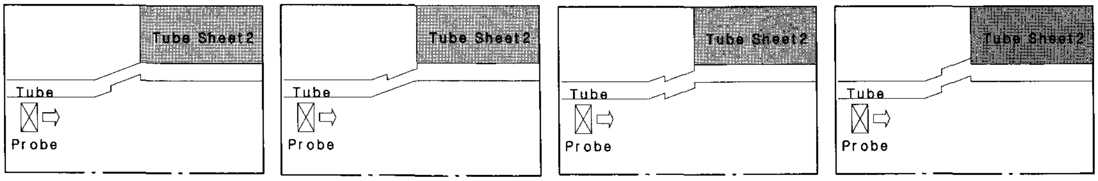

(a) ID (b) OD (c) Dent (d) Bulge

Fig. 10 Modeling situations of several different anomalies occurred on the transition region near tubesheet at P2 position

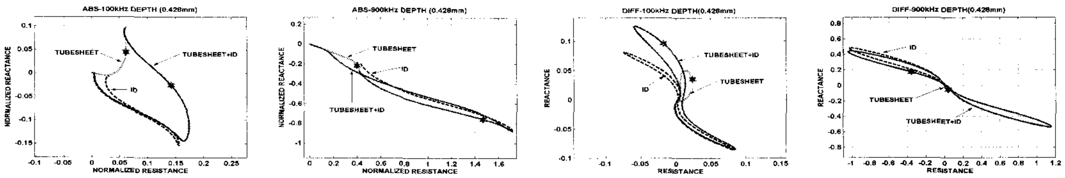

(a-1) 100 kHz Abs. ID (a-2) 900 kHz Abs. ID (a-3) 100 kHz Diff. ID (a-4) 900 kHz Diff. ID

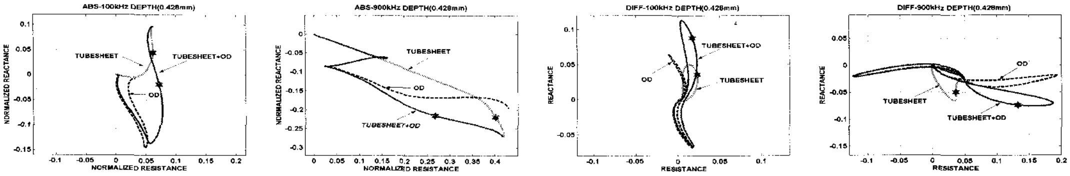

(b-1) 100 kHz Abs. OD (b-2) 900 kHz Abs. OD (b-3) 100 kHz Diff. OD (b-4) 900 kHz Diff. OD

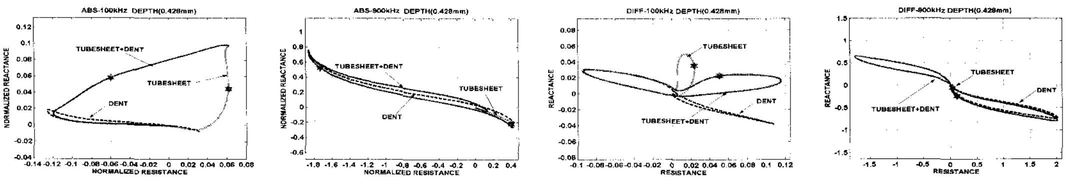

(c-1) 100 kHz Abs. Dent (c-2) 900 kHz Abs. Dent (c-3) 100 kHz Diff. Dent (c-4) 900 kHz Diff. Dent

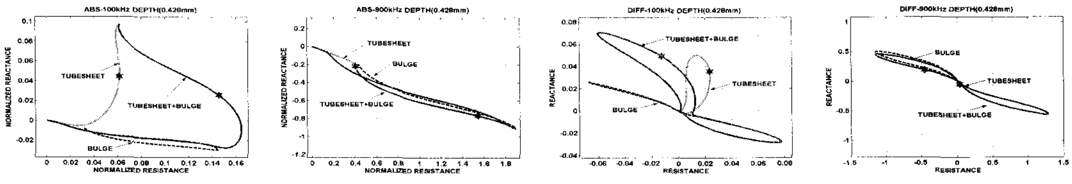

(d-1) 100 kHz Abs. Bulge (d-2) 900 kHz Abs. Bulge (d-3) 100 kHz Diff. Bulge (d-4) 900 kHz Diff. Bulge

Fig. 11 Absolute and differential signals from anomalies illustrated in Fig. 10 at low and high frequencies

Characteristics of Defect Signals under the Influence of Tubesheet and Tube Expansion Region

Fig. 10 shows modeling situations of several different anomalies occurred on the transition region near tubesheet at P2 position. The width and the depth of all anomalies are 10.272 mm and 0.428 mm, respectively. Fig. 11 shows absolute and differential impedance plane signals from anomalies illustrated in Fig. 10 at 100 and 900 kHz. According to these results, the tendency of vector addition of individual signals seems to exist at low frequency signals. This may be because the skin depth is deep enough at the low frequency to reflect all the outside environment and variations around TTS region. However, if we use high frequencies, the part of individual anomaly signal is exaggerated in the mixed signal, which is very difficult to analyze. Therefore, low frequency is found to be more useful to analyze the mixed signal.

5. Summary

In this paper, absolute and differential signals are computed for several different locations of tube expansion and signal variations due to tubesheet, tube expansion and operating frequencies are investigated. Results show that low frequency is good for detecting TTS location and high frequency is good for sizing of expanded tube diameter as well as the recognition of transition region. The use of 900 kHz, differential horizontal component signal would make it possible to recognize both ends of the transition region as well as TTS location. To inspect the anomalies at tubesheet and tube expansion region, low frequency is preferred and at low frequency signals, the tendency of vector addition of individual signals seems to exist.

Acknowledgment

This work has been supported by KESRI (R-2003-B-107), which is funded by MOCIE (Ministry of Commerce, Industry and Energy).

References

ASME (1986) *Eddy Current Examination Method for Installed Nonferromagnetic Steam Generator Heat Exchanger Tubing*, Section V, Article 8, Appendix I

Burnett, D. S. (1988) *Finite Element Analysis from Concepts to Application*, Addison-Wesley, Reading, Massachusetts, USA

Kong, C. S., Lee, S. C. and Shim, D. N. (2004) Quality Characteristics Comparison of Tube Expansion Process on the Steam Generator, Symposium on the Safety of Steam Generator, Vol. 3, pp. 155-164